Nanoscale

PAPER

View Article Online
View Journal | View Issue

Cite this: *Nanoscale*, 2023, **15**, 17494

Eliminating waste with waste: transforming spent coffee grounds into microrobots for water treatment†

Amit Kumar Singh, *‡[a] Tarini Basireddy ‡[b] and Jeffrey L. Moran *[a,c]

Water pollutants such as oil spills, industrial dyes, and microplastics threaten public health and aquatic ecosystems. There are considerable challenges in removing water contaminants using traditional methods. Several studies have been conducted in recent years to develop effective water purification materials. Despite this, the mass production of most materials is extremely challenging because they involve multiple intricate steps and sophisticated equipment. Herein, we report the facile synthesis of spent coffee ground (SCG)-derived magnetic microrobots, which we dub "CoffeeBots", to remove oil, organic dyes, and microplastic pollution from contaminated seawater. In order to meet eco-friendly, high-yield and low-cost requirements, iron oxide nanoparticles (IONPs) were deposited on biodegradable SCGs using green chemistry. The IONPs on CoffeeBots facilitate magnetic navigation and recycling, microswarm assembly, and ease of retrieval after water remediation tasks. CoffeeBots' intrinsic surface hydrophobicity enables efficient on-the-fly capture and removal of oil droplets and microplastics from contaminated water with remote magnetic guidance. CoffeeBots were also functionalized with ascorbic acid (AA@CoffeeBots) to remove methylene blue (MB) dye contaminants from polluted seawater. SCGs and AA act as bioadsorbent and reducing agent, respectively, for MB dye removal whereas magnetic propulsion enhances mixing and accelerates MB decolorization. These CoffeeBots can be recycled numerous times for removing oil spills, organic dyes, and microplastics from the seawater. CoffeeBots hold considerable potential as sustainable, recyclable, and low-cost remediation agents for water treatment in the near future.

Received 24th July 2023,
Accepted 17th October 2023

DOI: 10.1039/d3nr03592a

rsc.li/nanoscale

Introduction

Water pollution is one of the most pressing environmental issues faced by modern civilization, as the past few decades have seen an increase in anthropogenic water contamination.[1,2] Water pollutants from agricultural runoff, industrial waste, and sewage have increased water-borne diseases and health issues. These contaminants can also disrupt marine ecosystems, leading to declining biodiversity. Water contaminants adversely affect aquatic flora and fauna, impairing photosynthesis and increasing chemical oxygen demand. Moreover, uncontrolled discharge of polluted effluent into marine ecosystems can result in bioaccumulation that poses a threat to human health.

Among the various water pollutants, soluble organic dyes pose a significant hazard to water quality because they are generally toxic, non-biodegradable, and readily dispersed in water.[3,4] The textile, leather, paints and pigments, plastics, paper, food, and cosmetic industries discharge significant quantities of effluents containing dyes into rivers and lakes. In addition to endangering aquatic ecosystems, some of these dye pollutants have long-term mutagenic and carcinogenic effects on humans.

Along with industrial dye pollutants, the prevalence of microplastics (MPs) in water bodies has gained attention in recent years.[5,6] MPs are microscopic particulates less than five millimetres in size that originate primarily from the fragmentation of larger plastic objects and personal care products. MPs are capable of withstanding environmental stress, allowing them to endure and persist in aquatic environments for up to several hundred years. Additionally, MPs are capable of adsorbing hydrophobic organic compounds and heavy metals, facilitating their transportation across different locations.[6,7] In

[a]*Department of Mechanical Engineering, George Mason University, 10920 George Mason Circle, Manassas, VA 20110, USA. E-mail: asingh91@gmu.edu, jmoran23@gmu.edu*
[b]*Thomas Jefferson High School for Science and Technology, Alexandria, VA 22312, USA*
[c]*Department of Bioengineering, George Mason University, 10920 George Mason Circle, Manassas, VA 20110, USA*

†Electronic supplementary information (ESI) available: Details of materials and characterization, additional experiments and videos. See DOI: **https://doi.org/10.1039/d3nr03592a**

‡These authors contributed equally to this work.

recent times, microplastics have also entered the food chain, and researchers have uncovered their presence in various parts of human bodies including lungs, placenta, breast milk, and blood capillaries.[5]

Alongside industrial dyes and MPs, oil spills constitute a substantial cause of water contamination.[8,9] Oil spillage in water can occur because of offshore drilling activities, distribution pipelines located underwater, or shipwrecks. As floating oil droplets coalesce at the water's surface, they form a thick film, blocking sunlight penetration and oxygen exchange, affecting the delicate balance that aquatic life needs to flourish. The spillage of oil has a significant impact on the world economy, including damage to local habitats, reduction of fishery resources, and decline in tourism activities.

At present, water purification facilities employ expensive techniques which include filtration, flocculation, membrane-based separation processes, adsorption, activated sludge techniques and coagulation methods to separate water impurities.[10,11] Despite attempts to mitigate water pollution through various processes, complete elimination of all pollutants from effluents remains a challenging task. The conventional techniques of treating wastewater also have their shortcomings, including the need for substantial land area, high energy consumption and frequent maintenance.[10,11] The majority of developing countries lack access to potable water due to a dearth of affordable water treatment techniques. The limitations of the wastewater treatment process have prompted researchers to investigate affordable approaches for efficient water purification.[11]

Water treatment with self-propelled microrobots has gained traction in recent years.[12–16] Microrobots are miniature machines that transform external sources of energy, such as chemical reactions,[17–19] light,[20,21] sound,[22,23] or gradients of magnetic field,[24,25] electric potential,[26] or temperature[27] into motion. Using magnetic fields or ultrasonic waves, many of these minute devices can be steered remotely to capture targeted pollutants present in water bodies. Microrobots offer various benefits over conventional water treatment methods such as cost-effectiveness, efficient payload release, enhanced mass transfer of pollutant to the catalyst surface, and accelerated detoxification of water.[28] In recent times, microrobots have shown promising results in efficiently removing different forms of water pollutants which include but are not limited to microplastics,[29–33] oil spillage,[31,34,35] industrial dyes,[33,34,36] heavy metals,[36,37] antibiotics,[38,39] endocrine disruptors,[40–42] nerve agents,[43] as well as combating water-borne pathogens.[44]

In this context, we present a simple and affordable method for producing magnetically-driven microrobots, which we dub CoffeeBots, using eco-friendly spent coffee grounds (SCGs), for water treatment. Every year, coffee production and consumption result in millions of tons of SCG waste.[45] The SCGs obtained after coffee brewing are mainly composed of cellulose, lignocellulose and organic compounds, such as lipids, amino acids, polyphenols, caffeine, melanoidins, and polysaccharides.[46,47] Since they are widely available, SCG biowastes are a convenient and cost-effective starting material for making CoffeeBots. In previous research, coffee grounds subjected to carbonization at high temperature[48–51] or chemical modifications[52–56] showed potential for eliminating oil spills,[48,49,54] organic dyes,[50,52,55] endocrine disruptors,[57] antibiotics,[57,58] heavy metals[51,53,56] and MPs.[59] However, there remains an unmet need for a cost-effective manner to render SCGs amenable to magnetic manipulation and steering, which will enhance their degradation performance and enable magnetic recollection upon completion. Accordingly, in this study we develop a sustainable synthesis method for fabricating SCG-based CoffeeBots.

The few prior studies that have explored the synthesis of magnetic SCGs[60–65] generally used methods that involve harsh chemicals and/or complicated synthesis processes; moreover, to our knowledge, no prior study has exploited the motility of magnetic SCGs to improve their pollutant removal performance. Originally, magnetic IONP-based SCGs were synthesized by reaction of iron chloride salts with alkali solutions of high concentrations in the presence of SCGs.[60–62] More recent studies have demonstrated the synthesis of static magnetic SCGs in an alcohol medium using perchloric acid-based ferrofluids[63,64] or tetramethylammonium hydroxide (TMAH)-treated IONPs,[65] as both perchloric acid and TMAH pose serious health risks.

In contrast to previous work, here we introduce a safe, simple, green-chemistry approach to fabricating magnetic SCGs (depicted in Scheme 1A) and demonstrate a straightforward method for attaching ascorbic acid (AA) as a pollutant-degrading cargo. Previously, AA has been used as payload in drug delivery applications of self-propelling particles,[23] but its efficacy as a payload for degrading MB pollutants has yet to be quantified. While we also functionalized SCGs with IONPs in an ethanol medium, the present study differs from previous studies[63–65] in the following ways: (i) the IONPs were applied directly to SCGs without any chemical modification; (ii) we propose a mechanism behind the direct incorporation of IONPs in SCG matrix in ethanol medium, providing evidence *via* Fourier Transform-Infrared (FT-IR) spectroscopy; (iii) compared to previous studies,[63–65] we demonstrate enhanced degradation efficiency when CoffeeBots are driven and steered through the water with an external magnetic field; (iv) we demonstrate AA as a novel pollutant-degrading cargo loaded onto IONP-functionalized SCGs, demonstrating rapid elimination of MB within 30 min; (v) we exploit their magnetically-driven motion to achieve "on-the-fly" elimination of diverse contaminants, ranging from methylene blue (MB) dye to model microplastics and oil spills.

To efficiently coat SCGs with IONPs, we used ethanol as a medium instead of water. Because of ethanol's lower density, the lighter SCGs and heavier IONPs both sediment in this medium, allowing them to be more easily dispersed than in water (in which the SCGs would have remained at the surface). The coating process proceeds straightforwardly: the suspended SCGs in ethanolic IONPs solution can be left undisturbed for 2 h at room temperature; at the end of the reaction, the newly-formed CoffeeBots can be extracted with a simple magnet.

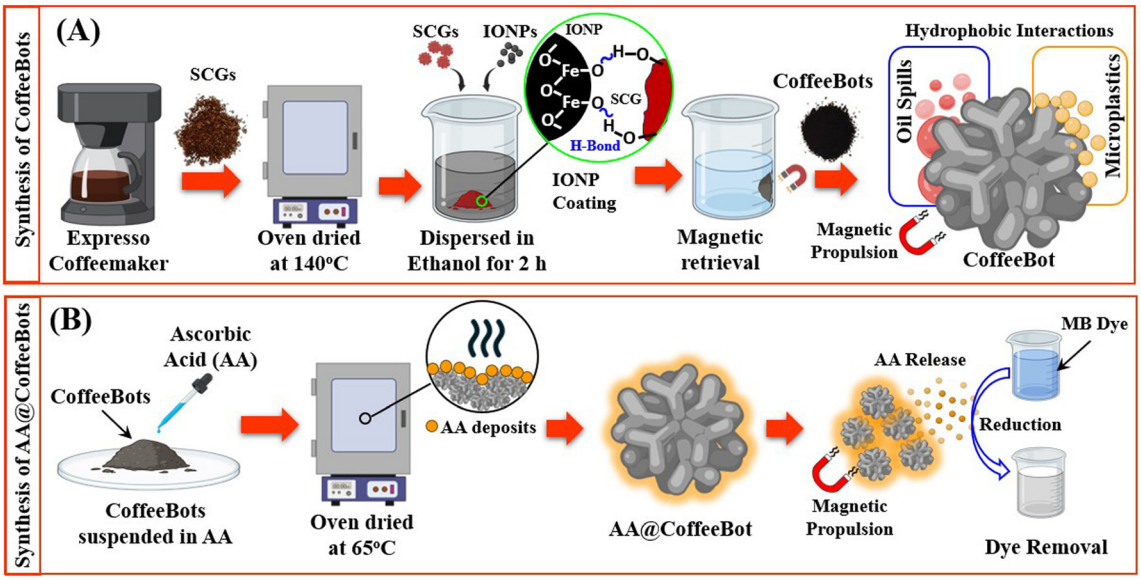

Scheme 1 (A) The SCGs were collected after brewing and desiccated in an oven. The dehydrated SCGs were immersed in an alcoholic mixture of iron oxide nanoparticles (IONPs) for 2 h. The IONPs bind to SCG surfaces as a result of hydrogen bonding between the oxygen elements in IONPs and hydroxyl (–OH) functional groups found on the surface of SCG. The CoffeeBots were retrieved using a magnet, and magnetically propelled CoffeeBots were used to clean up oil spills and remove microplastics (MPs) from seawater. Oil droplets and microplastic polystyrene (PS) particles adhered to the surface of the SCGs due to the hydrophobic interaction between the CoffeeBots and the pollutants. (B) The CoffeeBots were immersed in a solution of ethanol and water, which contained ascorbic acid, before being transferred to an oven. The CoffeeBots were coated with AA by evaporating the surplus solution. The CoffeeBots coated with Ascorbic acid (AA@CoffeeBots) were collected and utilized in dye removal experiments. The magnetically actuated microbots induce the release of Ascorbic acid, resulting in a decrease in methylene blue (MB) dye concentration.

This dispersion process provides an efficient way to render SCGs magnetically responsive. The interaction between the hydroxyl (–OH) functional groups of SCGs and oxygen entities of IONPs resulted in hydrogen bond formation, which ultimately led to a stable immobilization of these magnetic particles onto the surface of SCGs.[66,67] The magnetic actuation of CoffeeBots facilitated precise manipulation, navigation and retrieval after wastewater treatment. The CoffeeBots showcase their ability to restore polluted seawater through the elimination of organic dyes, microplastics, and oil spills. CoffeeBots are innately hydrophobic, which enables them to easily interact with microplastics and oil droplets. The magnetically-actuated CoffeeBots were able to successfully capture, transport and remove polystyrene (PS) microbeads as well as oil droplets that are suspended in seawater. This was accomplished by utilizing both the hydrophobic qualities of SCGs alongside the ferromagnetic nature of IONPs. In addition, magnetic microrobots were modified with ascorbic acid (AA), as shown in Scheme 1B, to facilitate the chemical reduction of water-soluble methylene blue (MB) dye pollutants present in seawater.

The CoffeeBots exhibit notable distinctiveness from the previously documented microrobots intended for water treatment in various aspects: (i) incorporating low-cost SCGs and biocompatible vitamin C or AA into a micro-robotic framework has been reported as a novel approach for water treatment. (ii) Instead of traditional iron salt reduction or chemically-modified IONPs for synthesis of magnetic SCGs, a green chemistry approach was applied to introduce unmodified IONPs into SCG wastes at room temperature. As a consequence, stable magnetic SCG residues were obtained without requiring any chemical reactions. (iii) The inherent hydrophobic properties of SCGs were utilized, without the need for extra chemical modifications or carbonization at high temperatures, to remove oil spills and microplastics. (iv) The CoffeeBots are equipped with multi-functional capabilities for water purification, including the ability to remove dye pollutants, oil spillage removal, and trapping of MPs contaminants.

Results and discussion

Characterization

We characterized the surface morphologies of uncoated SCGs and CoffeeBots using field emission scanning electron microscopy (FESEM). Fig. 1A and B show FESEM images of a ~450-μm uncoated SCG particle and CoffeeBot, respectively. Fig. 1C shows a magnified version of the same SCG depicted in Fig. 1A, revealing its surface morphology.

The uncoated SCGs have a rough, highly textured surface with heterogeneous porosity and flaky protrusions, resulting in a large specific surface area.[46,48,50,52] This feature makes them highly effective for water purification, as it enhances contact between the SCGs and the contaminants, resulting in

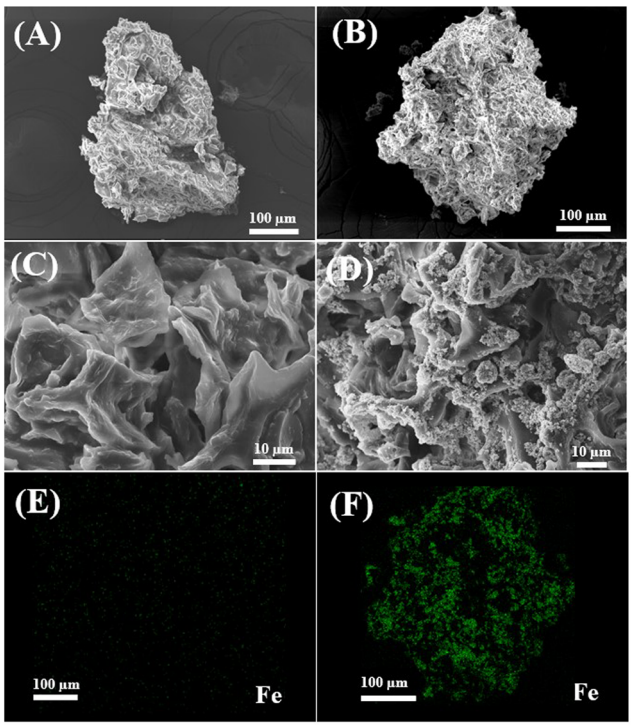

Fig. 1 FESEM micrograph of (A) uncoated SCG particle and (B) CoffeeBot. FESEM image of the surface morphology of (C) the uncoated SCG particle depicted in (A) and (D) the CoffeeBot depicted in (B). Panel (D) shows the presence of IONP aggregates on the flaky surface of SCGs. Elemental mapping of the SCG in (A) and CoffeeBot in (B), shown in panels (E) and (F) respectively, confirm the presence of iron (Fe) element on CoffeeBots.

a more efficient purification process. The Fig. 1D shows the surface morphology of a CoffeeBot, which clearly shows the distribution of IONPs on the flaky protrusions and surface of the SCG.[48,50] Fig. 1E and F show elemental mapping of iron (Fe) acquired *via* energy-dispersive X-ray spectroscopy (EDX) for an uncoated SCG and a CoffeeBot, respectively. As expected, there is no discernible sign of Fe in the uncoated IONPs, but for the CoffeeBots, there is a large quantity of Fe present throughout the surface area. This finding confirms that functionalization of SCGs with IONPs to form CoffeeBots has been successfully achieved. A further EDX analysis of the uncoated SCGs (Fig. S1B, refer to ESI†) showed that SCGs are composed mainly of carbon (C), nitrogen (N), sulfur (S), and oxygen (O) elements.[48,52] The EDX analysis of the CoffeeBots (Fig. S1D, refer to ESI†) showed the presence of elemental C, N, O, and S as the constituents along with a presence of metallic Fe from IONPs on the CoffeeBot surface. The FESEM images further revealed that the observed IONP aggregates are comprised of roughly spherical IONPs (Fig. S1E, refer to ESI†) of diverse sizes varying from 200–700 nm. Dynamic light scattering (DLS) measurements were conducted to revalidate the size distribution of the commercial IONPs, and the observations were reported in Fig. S1F of ESI.† Furthermore, the CoffeeBots exhibit a hierarchical microporous structure on their surface, with pore sizes ranging from approximately 0.5 to 70 μm (refer to Fig. S2 of ESI†). This structure results in a porosity of about 70.4%, as determined using a pycnometer. Moreover, contact angle measurements revealed that the CoffeeBots display significant hydrophobicity without any surface alterations required (Fig. S3, refer to ESI†).[48]

To determine the surface charge characteristics of the SCGs and IONPs, the zeta potential was measured using electrophoretic light scattering (ELS). The mean zeta potential values of uncoated SCGs, IONPs, and CoffeeBots are demonstrated in Fig. S4 of ESI.† In 0.1× phosphate buffered saline (PBS) buffer, the zeta potentials of uncoated SCGs[56] and free IONPs were measured to be −21.7 ± 1.5 mV and −62.3 ± 5.6 mV, respectively. Compared to uncoated SCGs, the coating of negatively charged IONPs enhanced the negative surface charge on the CoffeeBots, with a measured value of −42.7 ± 2.5 mV. The chemical durability tests further demonstrated that CoffeeBots retained their hydrophobicity when exposed to corrosive liquids and salt solutions (Fig. S5, refer to ESI†).

Since both SCGs and IONPs possess negative charges, we inferred that the binding affinity of IONPs to SCGs did not occur through electrostatic attraction. The evidence strongly indicates that different intermolecular forces, such as hydrogen bonding, are responsible for the attractive interactions between SCGs and IONPs.[66,67]

To gain a deeper understanding of the interactions between SCGs and IONPs, we performed Fourier transform-Infrared (FTIR) spectroscopy on SCGs alone, IONPs alone, and CoffeeBots. The FTIR spectrum of bare SCGs, shown in Fig. 2A, exhibits all the distinctive peaks that are consistent with previously published literature.[46,47,55,56] The distinct peak at 3487 cm^{-1} is associated with the stretching vibration of free

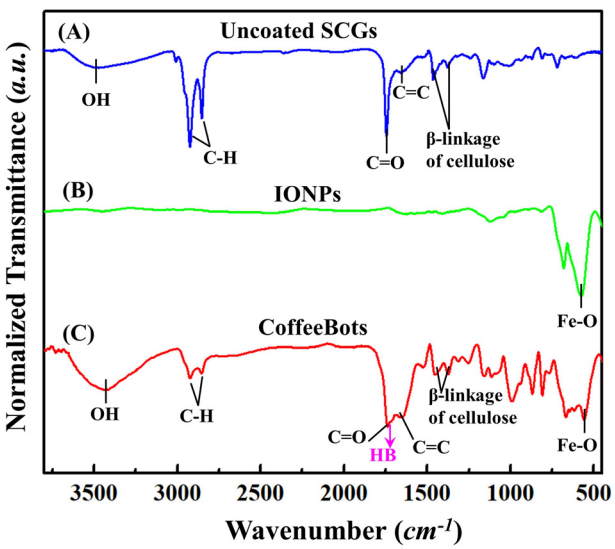

Fig. 2 Normalized FTIR spectra of (A) uncoated SCGs, (B) IONPs and (C) CoffeeBots. The signal observed at 1712 cm^{-1} position in (C), represented by the magenta-coloured arrow, suggests the presence of hydrogen bonded (HB) carbonyl groups in CoffeeBots.

or intermolecular bonded hydroxyl (–OH) groups arising from alcohols, phenols, and carboxylic acids, which constitute the hemicellulose, cellulose, and lignin known to be present in SCGs. The distinct peak at 2926 cm^{-1} is attributable to asymmetric and symmetric stretching of C–H bonds present in methylene ($–CH_2–$) and methyl groups ($–CH_3$), respectively. The occurrence at 2855 cm^{-1} implied stretching of aliphatic C–H bonds deriving from the cellulose backbone. The peaks observed at 1746 cm^{-1} and 1652 cm^{-1} pertain to the stretching vibrations of carbonyl (C═O) and carbon–carbon double bonds (C═C), respectively. These vibrational modes are associated with caffeine, hemicellulose, and chlorogenic acid molecules. The peaks located at 1471 cm^{-1} and 1370 cm^{-1} is ascribed to the β (1 → 4) linkage in non-crystalline cellulose. In the FTIR spectrum for IONPs (Fig. 2B), the vibrational bending of Fe–O in magnetite (Fe_3O_4) accounted for the peaks observed at 678 cm^{-1} and 568 cm^{-1}.[49,50]

Fig. 2C displays the FT-IR spectrum of the CoffeeBots. These data demonstrate that introduction of IONPs to the SCGs resulted in a marked shift in the –OH peak from 3487 cm^{-1} to 3432 cm^{-1}. The alteration suggests that the –OH functional groups present in SCGs play a role in binding with IONPs.[66,67] Within the widened C═O spectral absorption band at 1741 cm^{-1} for CoffeeBots, a weak peak appears around 1712 cm^{-1}, as exhibited in Fig. 2C. However, this peak appears neither in the pure SCG nor in the pure IONP spectrum. Previous studies have shown that signals related to weak hydrogen bonding associated with carboxylic groups may be seen around ~1710 cm^{-1}.[66–68] Thus, the weak peak signal observed at 1712 cm^{-1} might be ascribed to the stretching vibration of hydrogen-bonded carbonyl (C═O) groups.[58,66–68] The alteration observed in the –OH peak, widening of C═O peak, and appearance of a peak around ~1712 cm^{-1} may explain the interaction occurring between the oxygen (O) moieties of IONPs and the functional groups bearing hydroxyl (–OH), namely alcohols, phenols, and carboxylic acids, that are present in SCGs.[66,67] The peaks for C–H (2922 and 2850 cm^{-1}), C═C (1648 cm^{-1}), and β (1 → 4) linkage of cellulose (1455 and 1370 cm^{-1}), arising from SCGs were present in the FT-IR spectrum of CoffeeBots, while the peak at 562 cm^{-1} is indicative of Fe–O vibrational bending of the incorporated IONPs.

Motion control experiments

The speed and direction of the moving CoffeeBots can be precisely controlled by an external magnetic field. Consequently, the CoffeeBots could effortlessly alter their spatial paths, simply altering the orientation of a bar magnet.[31] Furthermore, the CoffeeBots are capable of operating at high speeds and following intricate paths, making them ideal for water purification applications. Fig. 3(A–D) and Video S1† illustrate the motion (driven by an external NdFeB magnet) of CoffeeBots in the vertical and horizontal directions. In addition, Fig. 3(E–G) and Video S2† further illustrate magnetically-driven motion in a prescribed direction along a path that follows the letters G, M, and U. Videos S1 and S2† together demonstrate accurate manipulation of CoffeeBots' magnetic

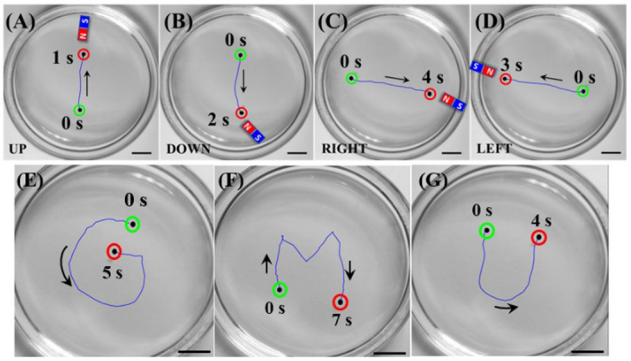

Fig. 3 Precise migration of the CoffeeBot (~450 μm) through magnetic guidance in seawater. The controlled magnetic navigation was used to migrate the CoffeeBot in (A) upward (B) downward (C) right and (D) left directions. (E–G) The CoffeeBot was also magnetically actuated in G, M and U trajectories. The numbers depict the instantaneous position of the CoffeeBot at different time intervals. The scale bar shown is of 5 mm length. The black arrows and the numbers in all images denote motion direction and the time in seconds, respectively. Green and red circles represent the initial and final positions of the CoffeeBots.

navigation in seawater. CoffeeBots require only a magnetic field to move, which is an advantage when operating in seawater, since the high ionic concentrations severely restrict the self-propulsion of several fuel-based microswimmer designs under these conditions.[69–72] In addition, we investigated how variations in magnetic field intensity affected the linear speed of the microrobots.

Fig. S6 in ESI† depicts the variation of speed of microrobots with the increase in magnetic field strength. To identify the salient features of the magnetically induced motion, a series of experiments was performed employing a ~450 μm CoffeeBot inside a bath of seawater.

The velocity of the CoffeeBots increased significantly with the increase in magnetic field intensity, achieving a maximum velocity of ~5500 μm s^{-1}, equivalent to ~12 body lengths per second, at 95 mT of magnetic field strength (Fig. S6, refer to ESI†).

Organic dye decontamination

As a model chemical pollutant, we chose to remove the cationic dye methylene blue (MB) from seawater using CoffeeBots under ambient conditions. MB is widely used as a colorant in the textile industry. First, the absorbance of MB dye solutions was characterized as a function of concentration (0–12 mg L^{-1}) to create a calibration plot for quantitative analysis of dye decontamination. In alkaline seawater (pH ~ 8.1), MB molecules exhibit intense absorption bands between 200–700 nm with a maximum (λ_{max}) at 665 nm.[50,55] This calibration plot revealed a linear relationship between MB concentration and corresponding absorption peak intensities at 665 nm (Fig. S7, refer to ESI†) and was used in the rest of our MB removal experiments.

A recent study by Benmaamar *et al.*[73] found that the effectiveness of SCGs for MB dye removal through absorption increases with increasing alkalinity. The researchers observed

that SCGs acquired negative charges when the media pH was basic, enabling them to electrostatically attract cationic MB molecules.[73,74] Additional previous studies indicate that MB molecules and anionic SCG particles interact *via* hydrogen bonding and electrostatic attraction during the absorption process.[74,75] Hence, due to their intrinsic negative surface charge, CoffeeBots are capable of electrostatic interactions with cationic MB dyes, and the presence of hydroxyl (–OH) groups results in hydrogen bonding with MB moieties, resulting in MB absorption (Fig. 4A).[74,75] In this context, 50 mg of CoffeeBots were suspended in 8 mL of MB solution (10 mg L^{-1}) in seawater. To estimate the MB removal rate, the aliquots were drawn at respective time intervals and the absorbance of the samples was measured at λ_{max} = 665 nm using a Tecan microplate reader. Fig. 4(B and C) showed that after 40 min of treatment, motile CoffeeBots depleted the MB concentration from 10 mg L^{-1} to ~5.39 mg L^{-1}, which corresponds to ~46% of dye removal. Control experiments were conducted by suspending 50 mg of uncoated SCGs in 8 mL of 10 mg L^{-1} MB solution. A 40 min treatment with uncoated SCGs decreased the MB concentration from 10 mg L^{-1} to ~5.2 mg L^{-1}, corresponding to ~48% dye removal. There were no significant differences between dye removal efficiency using uncoated SCGs and CoffeeBots. The dye removal rate with a rate constant of ~0.016 min^{-1} was recorded for both uncoated SCGs and CoffeeBots treatments (Fig. S8, refer to ESI†). The decrease in MB concentration in both the cases can be attributed to the absorption of MB on the surface of the SCGs and CoffeeBots for 40 min treatment. In the presence of indoor light, the MB dye solution remained stable after 40 min without particles (No SCGs), negating the role of light-induced degradation.

For AA@CoffeeBots, the negative surface charge of the CoffeeBots facilitates the MB reduction, while the autonomous release of AA in seawater accelerates the rate of MB decolourization (Fig. 4A). The high MB removal rate can mainly be attributed to the reduction of MB dye by ascorbate ions (As^{2-}).[76–78] Recently, the MB/As^{2-} redox system has been used for the clinical investigation of ascorbic acid concentration in blood serum.[79,80] The chemical process involving the reaction of MB and AA is commonly recognized, and prior research has thoroughly examined the speed at which MB undergoes reduction *via* AA under diverse levels of pH and temperature. In the aforementioned process, it can be observed that upon interaction with AA molecules, the MB gets converted into its reduced state, known as leucomethylene blue (LMB or MB_{red}). While this process is taking place, AA is being oxidized, which

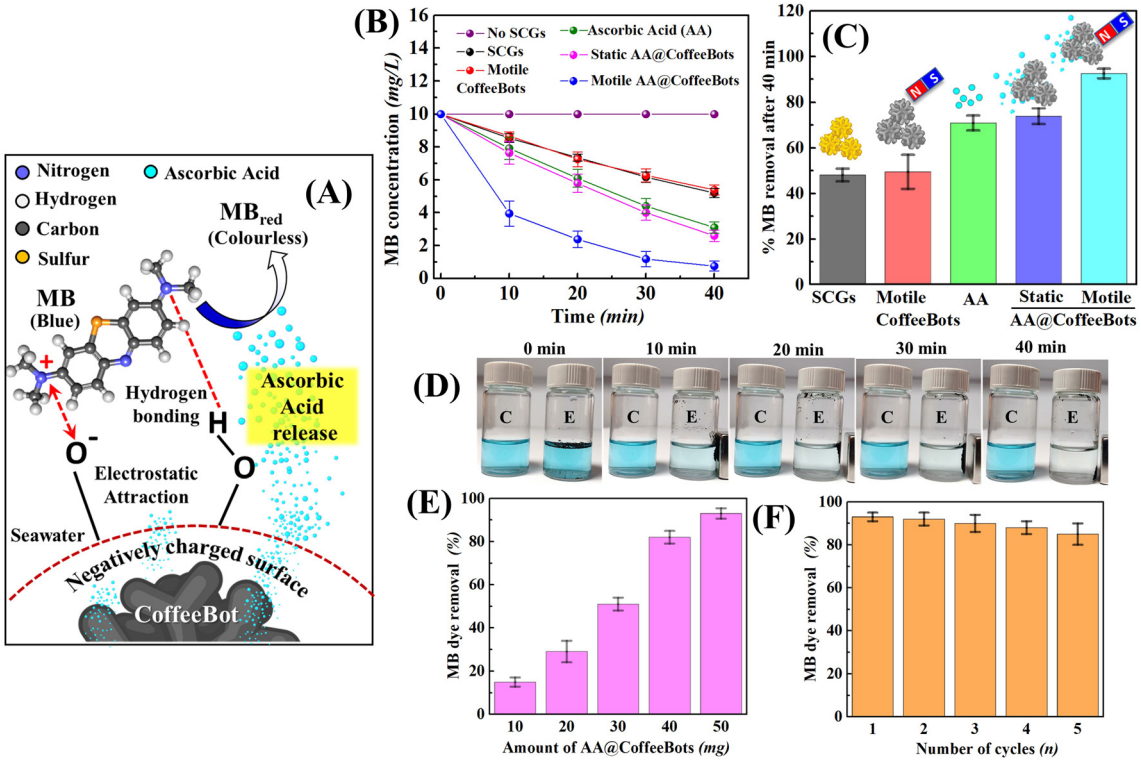

Fig. 4 (A) Schematics showing the interaction between negatively-charged SCG particles and cationic MB molecules. The release of ascorbic acid (AA) from the surface of AA@CoffeeBots speeds up the dye removal by rapid MB reduction in seawater. (B) Variation in MB concentration in seawater over time in the absence of any particles and in the presence of SCGs, motile CoffeeBots, AA only (no SCGs or CoffeeBots), and stationary or motile AA@CoffeeBots. (C) Percent removal of MB after 40 min. (D) Removal of MB from seawater by magnetically actuated AA@CoffeeBots (50 mg) over a 40-minute period. The control vial (denoted by C in the image) and experimental vial (denoted by E) were placed side by side, and the CoffeeBots were pinned against the wall with a magnet before capturing the images. (E) Percent dye removal after 40 min for different amounts (mg) of AA@CoffeeBots. (F) Reusability of AA@CoffeeBots (50 mg) for removal of MB dye from seawater.

results in the formation of dehydroascorbic acid (DHA). The disappearance of the blue colour in the MB solution is attributed to the formation of colourless MB_{red} moieties (Fig. S9, refer to ESI†).

Nevertheless, MB_{red} can undergo oxidation leading to its conversion back into MB and consequently recovering the characteristic blue hue. According to prior research, an excess of As^{2-} ions in MB solution with a pH just above neutral can adjust the equilibrium kinetics in favour of product formation. This change restricts the conversion of MB_{red} molecules back into their initial state. To impede the transformation of MB_{red} into MB, and accomplish total reduction of MB, it was necessary to excessively coat CoffeeBots with AA. In this regard, CoffeeBots were coated with an excess amount of AA which equals ~3.3 mg of AA for each mg of the CoffeeBots. Subsequently, AA@CoffeeBots were immersed into 8 mL of seawater polluted with 10 mg L^{-1} MB dye, and the microrobots were rendered stationary or static by placing a bar magnet near the reaction vessel. For motile AA@CoffeeBots, a bar magnet was used to steer the microrobots in the reaction vessel for 40 min. A rapid discoloration of the dye took place in a span of 40 min by administering motile AA@CoffeeBots. As shown in Fig. 4(B and C), free AA molecules reduced the MB concentration from 10 mg L^{-1} to ~3.1 mg L^{-1}, which corresponds to ~70% of dye removal and rate constant of ~0.029 min^{-1} (Fig. S8, refer to ESI†). Fig. 4(B and C) depicts that stationary and motile AA@CoffeeBots reduced the MB concentration from 10 mg L^{-1} to ~2.65 mg L^{-1} and ~0.75 mg L^{-1} after 40 min treatment, which corresponds to ~74% and ~93% of dye removal, respectively. Thus, magnetically-driven motion resulted in improved transport of AA molecules to the CoffeeBots' surfaces and mixing of reactants during movement, leading to enhanced efficiency of MB removal.[24,34]

Furthermore, Fig. 4D and Video S3† demonstrates the time-dependent MB reduction using 50 mg of motile AA@CoffeeBots suspended in 8 mL seawater containing 10 mg L^{-1} MB dye. CoffeeBots were veered into vials by controlling the orientation of a bar magnet, and they were easily retrieved after remediation. According to reports by El-Aila,[76] the MB reduction in presence of excess ascorbate (As^{2-}) moieties is proportional to the concentration of AA in mildly basic environment, such as seawater (pH 8.1) in this work, indicating adherence to first-order reaction. A rate constant of ~0.034 min^{-1} was observed for stationary AA@CoffeeBots and ~0.072 min^{-1} for motile AA@CoffeeBots (Fig. S8, refer to ESI†). At any given point in time, static CoffeeBots removed less MB than their motile counterparts.[34,41] These results indicate that the magnetically-driven motion of CoffeeBots enhances mass transfer of MB to the SCGs' surfaces. Consequently, the magnetic actuation of CoffeeBots enhanced the MB dye elimination process.

Fig. 4E demonstrates the elimination of MB from seawater by employing varying quantities of AA@CoffeeBots. After 40 min of treatment, 50 mg of AA@CoffeeBots removed ~93% of MB dye, whereas 10 mg of AA@CoffeeBots only managed to remove about 15% of the MB dye. The study findings indicated a positive correlation between the number of remediation agents and removal efficiency. The maximum removal efficiency was observed when microrobots were used at an amount of 50 mg in 8 mL of 10 mg L^{-1} dye.

Moreover, 50 mg of AA@CoffeeBots underwent successive MB removal trials over five rounds to assess their capacity for reuse in eliminating a concentration of 10 mg L^{-1} from seawater within a treatment duration of 40 min. The experimental details for the regeneration of AA@CoffeeBots have been stated in the ESI.† Fig. 4F shows the results of the reusability tests of AA@CoffeeBots for removal of dye contaminants. After each experimental cycle, AA@CoffeeBots were magnetically retrieved from seawater and regenerated (refer to ESI†). After five cycles, about ~8% loss of MB dye decontamination efficiency was observed in this study. The results showed that the microrobots retained their efficiency for removing MB dye even after multiple cycles, suggesting that they could be reused effectively after repetitive AA functionalization.

Spill cleanup and recovery

Microswimmers have been integrated with hydrophobic entities such as self-assembled alkanethiols, long oleic acid chains, organic indigo dyes,[81] surfactants, stearic acid surface coatings, pollen grains,[31] and carbon soot[34] over the past decade to selectively capture, transport, and remove oil contaminants from aqueous environments.[35] The majority of these microrobots have been manufactured using sputter coating, electrodeposition, or chemical modification and utilize toxic fuels in conjunction with a magnetic field or surface tension gradient for locomotion.[35] CoffeeBots have a distinct advantage over other oil recovery micromotors in that they consist of sustainable SCG biowaste with inherent hydrophobicity and do not require any fuel, nor do they require physical deposition or chemical reactions for synthesis.[34] The ability of CoffeeBots to remain buoyant on the water surface reduces drag and improves oil/water separation efficiency due to their hydrophobic interaction with floating oil droplets. In addition to enabling magnetically-driven motion, which as demonstrated above increases removal efficiency, the presence of magnetic IONPs on the CoffeeBots' surface facilitates on-demand recovery of the oil contaminant-laden SCGs.

We conducted experiments to test the ability of the CoffeeBots to remove floating oil droplets from seawater, using automotive oil as a model of an oil spill. Unlike some previous microswimmer-based oil recovery studies,[35,82] no surfactants or fuels were needed, and the alkalinity of seawater (pH 8.1) was not altered in order to simulate the real scenario of oil pollution in seawater. Fig. 5 depicts the magnetic actuation of CoffeeBots in seawater for effective capture and transport of free-floating oil droplets. A ~400 μm CoffeeBot was employed to retrieve an oil droplet of nearly the same size (~528 μm) drifting freely in seawater. Fig. 5A and Video S4† show a CoffeeBot directed towards a floating oil droplet using a hand-held bar magnet. After contacting the oil droplet, CoffeeBots capture and transport it along the predesigned path with high precision. The micromotor was re-oriented by adjusting the

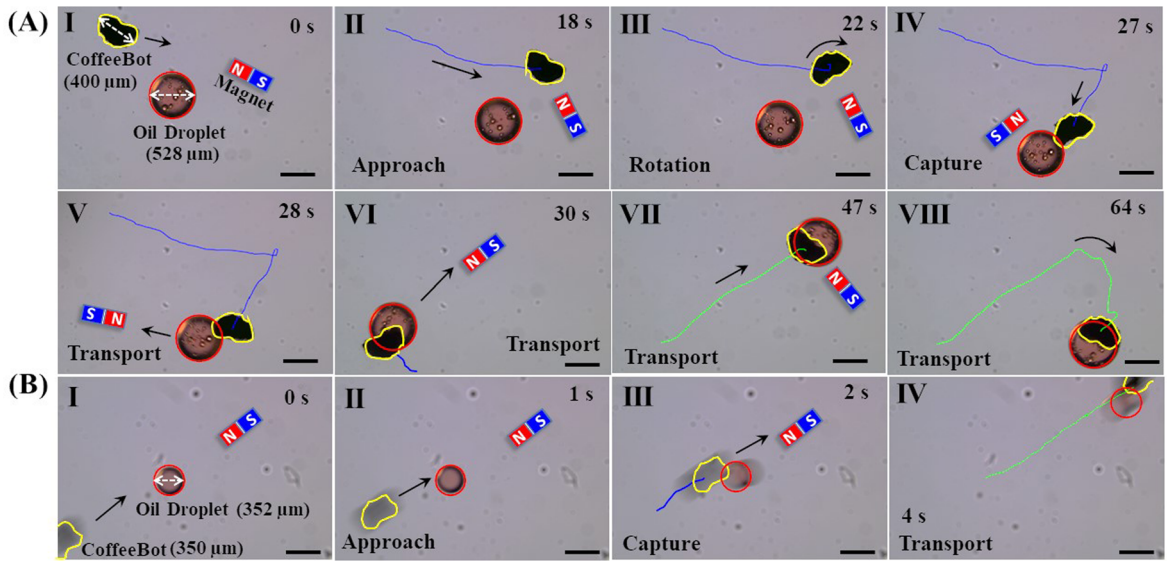

Fig. 5 Magnetic guidance of a CoffeeBot to capture oil droplets in seawater. The Image set (A) shows the approach, capture, and transport of a free-floating oil droplet by a CoffeeBot under precise magnetic control. The images (B) shows the oil spill capture by a magnetically actuated CoffeeBot moving at high speed in linear trajectory. The blue and green lines show the trajectory of the motor before and after capture of oil droplets, respectively. Scale bars in all panels represent 400 μm. The black arrows and the numbers in all of the images denote the direction of motion and the time in seconds, respectively. The oil droplets are labeled with a red circle, and CoffeeBots are indicated with yellow borderlines.

position of the magnet, followed by capture and conveyance under precise magnetic control. The inherent hydrophobicity of SCGs facilitated a strong hydrophobic interaction between the oil droplets and motor surface.[34] Upon coming into contact with the free-floating oil droplets, the hydrophobic CoffeeBot immediately absorbed the oil droplets onto its surface. As the CoffeeBot transported the oil droplet from one location to another under the influence of the magnetic field, the oil droplet engulfed the SCG and they moved together as a single entity. Additionally, Fig. 5B and Video S5† depicts that the CoffeeBot collects an oil droplet at a remarkable speed. The magnetically navigated CoffeeBot (~350 μm) captured a stationary oil droplet (~352 μm) while travelling at high speed up to ~600 μm s^{-1}, which corresponds to ~1.7 body lengths per second, whereas the droplet remained anchored to the motor surface while in motion. This observation suggests that CoffeeBots can reliably collect oil droplets, as the interacting hydrophobic forces prevent oil droplets from dislodging during rapid locomotion.

Furthermore, a collection of CoffeeBots (8 mg) of varying size, ranging from 300–450 μm, were deployed in a Petri dish (9 cm diameter) to demonstrate retrieval of floating oil contaminants on a macroscopic scale. The disc-like CoffeeBotic swarm was magnetically actuated in 20 mL of seawater to capture a macroscale oil drop with a diameter of 0.6 cm. Fig. 6 and Video S6† depict the oil spillage removal operation by a swarm of CoffeeBots under the influence of external magnetic field. By utilizing magnetic forces, the magnetic swarm navigated towards the affected area simultaneously to remove the oil spill. The CoffeeBotic swarm successfully absorbed the entire oil spill by hydrophobic interaction in a fraction of seconds, as shown in Fig. 6(B–E).

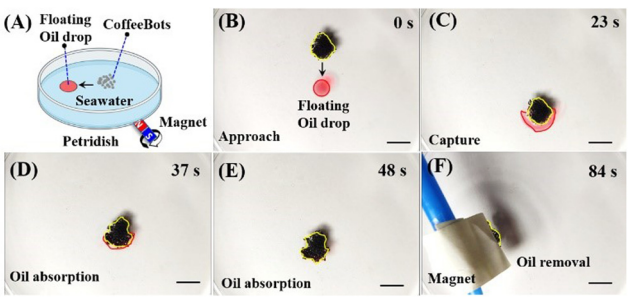

Fig. 6 Oil droplet manipulation by swarming of magnetic CoffeeBots on a macroscopic scale. Image (A) shows the experimental set-up for oil capture and the position of the external magnetic field for magnetic guidance of swarm in seawater. Image (B–E) shows motion of the CoffeeBotic swarm in the presence of a bar magnet. Image (F) shows the magnetic retrieval of the CoffeeBotic swarm after oil spill absorption. Scale bars in all panels represent 1 cm. The black arrow and the numbers in all of the images denote the direction of motion and the time in seconds, respectively. The oil droplets are encircled in red lines, and CoffeeBotic swarms are indicated with yellow borderlines.

The collective behaviour of the microswarm demonstrated the ability to actuate by remote magnetic field, remove oil spills, and create localized hydrophobic interaction with oil spill while in motion. Moreover, the magnetic microswarm could even be retrieved on-demand by an external bar magnet after the end of the oil removal operation (Fig. 6F).

Oil slicks are difficult to remove compared to oil droplets because they form a cohesive layer that spreads over a large area across the surface of the water, posing serious threats to aquatic ecosystems. To address this issue, a magnetic swarm (40 mg) comprising of varying size CoffeeBots, ranging from

300–450 μm, were deployed in a 10 mL beaker to retrieve a floating oil slick from the surface of the seawater.

The oil sample (30 μL) was placed on the surface of seawater in a beaker, generating two distinct phases which replicates an oil spill scenario without emulsification. Fig. 7(A–F) and Video S7† show the oil slick removal experiment using CoffeeBots as a biosorbent material. As shown in Fig. 7(B–E), oil sorption happens quickly, within 2 min of CoffeeBots-oil interaction, *via* hydrophobic interactions with the CoffeeBots' surface and the freely floating oil slick.

Most oil recovery materials in use today, which are typically composed of activated charcoal and biochar, tend to settle to the bottom after oil absorption as their densities exceed that of water. Consequently, recovering these materials after oil absorption treatment is challenging. In contrast, the CoffeeBots absorb oil rapidly enough to form a clump or "oil tar" and remain buoyant in seawater. The CoffeeBotic swarm could be separated easily from the surface of seawater using a bar magnet (Fig. 7F). At the end of the operation, the CoffeeBots were easily recovered by a bar magnet as an alternative to filtration.

To investigate the oil absorption capability and reusability of the CoffeeBots, the oil separation efficiency (OSE) was determined by a series of experiments (Fig. 8). Fig. 8A demonstrates the oil separation efficiency or OSE (%)[34] of the varying amounts of CoffeeBots (in mg) when subjected to the removal of oil slicks, for a time span of 3 min. The results of this study showed that OSE increased monotonically with the increment in the amount of CoffeeBots (in mg) subjected to oil decontamination (Fig. 8A). It was found that 5 mg of CoffeeBots were successful in removing ~31% of oil contamination as a result of the operation. In addition to increasing the number of CoffeeBots beyond 5 mg, we also found that when 30 mg of micromotors were used for a prolonged period of 3 min, the OSE improved to ~99%.

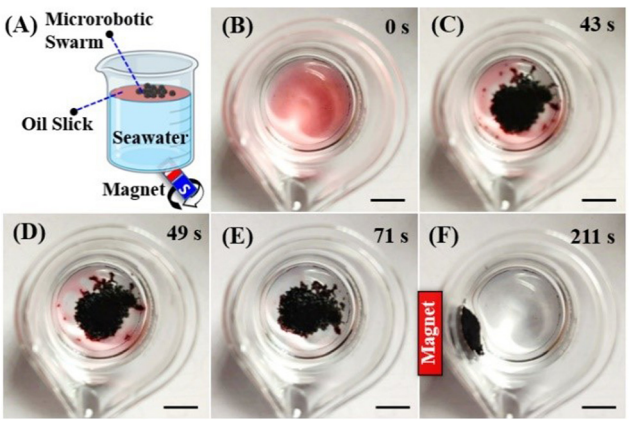

Fig. 7 Oil slick absorption by collective behaviour of CoffeeBots. (A) The experimental set-up for oil slick capture is shown along with the position of the permanent bar magnet for magnetic guidance of the swarm. The images (B–E) show the absorption of floating oil slick by CoffeeBots' swarm. (F) After oil slick absorption, the swarm was magnetically retrieved and pinned to the wall of the beaker. Scale bars in all panels represent 1 cm. The numbers in all of the images denote the time in seconds.

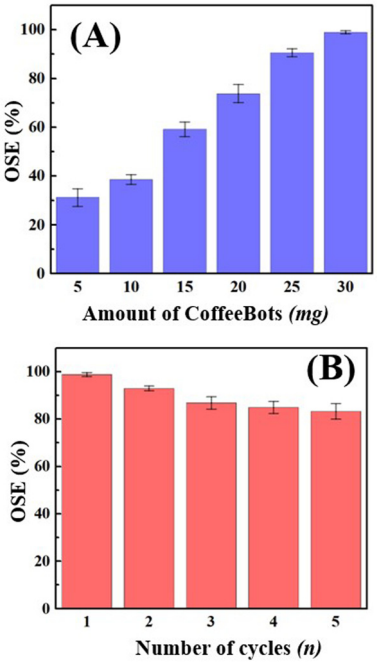

Fig. 8 (A) Oil separation efficiency or OSE (%) for varying amount (mg) of CoffeeBots for oil contaminant removal. (B) Recycling performance of CoffeeBots for removal of oil contamination.

Further, the exhausted CoffeeBots were regenerated for successive oil recovery experiments. The methods for regeneration of CoffeeBots after oil recovery have been specified in the ESI.† Fig. 8B shows the results of the reusability tests of a swarm of CoffeeBot (30 mg) for removing oil contaminants after 3 min treatment. After each separation experiment cycle, exhausted CoffeeBots were washed with acetone to remove the absorbed oil.

For successive cycles, the CoffeeBots are reintroduced into the oil–water two-phase mixture. The results show that the CoffeeBots maintained their absorption efficiency above ~80% after five cycles. However, it was observed that OSE declined by about ~15.6% after five cycles. This suggests that the CoffeeBots retained their functional integrity even after multiple separation cycles. However, CoffeeBots, were unable to remove oil emulsions that had been dispersed in seawater and stabilized with surfactant. The hydrophobicity of CoffeeBots can be further enhanced by functionalizing them with additional superhydrophobic entities[83–85] to remove surfactant-stabilized oil emulsions. Since this work focused on the facile synthesis protocol, the functionalization of CoffeeBots with superhydrophobic entities is left for future work.

Microplastics trapping

Microrobots have been extensively studied as potential tools for eliminating microplastic pollution in recent years. Most of the reported microrobots are engineered to remove microplas-

tics (MPs) *via* absorption, precipitation, electrostatic and phoretic interactions.[29–33,86] The CoffeeBots rely on their intrinsic hydrophobicity without further surface modifications for MPs removal from seawater. Yen and co-workers[59] have shown the potential of uncoated SCGs for removal of nanoplastics (NPs), in the form of fluorescent-orange amine-modified polystyrene beads (fluo-NP). The researchers in that study have attributed the SCGs' ability to collect the fluo-NPs to hydrogen bonding between the amine group of fluo-NP and the hydroxyl and carboxyl groups on SCGs.[59] In this work, CoffeeBots were deployed for the removal of extremely fine unmodified polystyrene (PS) microbeads from seawater. PS were selected as model MP pollutant as previous studies found that PS microparticles account for 10% of the plastic particles in untreated water and sediment. To analyse the feasibility of clearing MP pollutants, CoffeeBots were mixed with PS microspheres in seawater and exposed to a magnetic field. The physical adsorption of the MPs on the CoffeeBots was observed under an optical microscope. Fig. 9 and Video S8† depict the magnetic field-driven motion of a CoffeeBot and dynamic removal of spherical PS microbeads. MPs have been found to exhibit a strong affinity towards hydrophobic water contaminants, according to previous studies. In this manner, the inherent hydrophobicity of SCGs makes them ideal to serve as adherence sites for mounting MPs on the surface of the microrobots.[6,7] In our study, CoffeeBots demonstrates physical absorption of PS beads governed by their hydrophobic interaction (Fig. 9A). CoffeeBots and PS beads exhibit nearly equal zeta potentials of −42.7 ± 2.5 mV and −42.1 ± 2.9 mV, respectively, which negates the chances of electrostatic attraction between them (Fig. S3, refer to ESI†). Fig. 9(B–E) shows a time-lapse of a CoffeeBot (~380 μm in size) approaching, capturing and transporting an assembly of spherical PS microbeads under magnetic actuation. PS microbeads attach to the CoffeeBot's surface (Fig. 9F) and are dragged along by a bar magnet under magnetic field guidance.

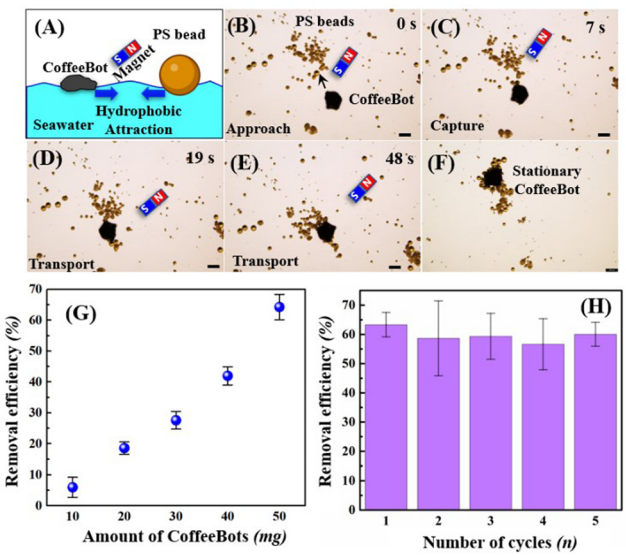

Fig. 9 (A) Magnetic propulsion of CoffeeBots for polystyrene (PS) bead capture *via* attractive hydrophobic interaction. Time-lapse images show (B) CoffeeBot approaching an assembly of PS microbeads, (C) capture of PS microbead cluster by magnetically actuated CoffeeBot, (D and E) transportation of adhered microplastics under magnetic field. (F) Stationary microrobot taken after 10 min of microplastic capture operation. The scale bar is 200 μm in all images. Plot (G) shows CoffeeBot mass-dependent removal efficiency of PS beads from seawater and (H) depicts the recycling performance of CoffeeBots for removal of PS beads.

The buoyant CoffeeBots can effectively capture and transport these floating MPs under magnetic guidance. In a series of experiments, different quantities of CoffeeBots were employed to quantify the removal of MPs through hydrophobic interactions. Fig. 9G demonstrates that as the quantity of CoffeeBots (in mg) used in the microplastic PS bead decontamination increased, there was a corresponding rise in removal efficiency. We observed that 10 mg of CoffeeBots removed only ~6% of PS beads after 1 h treatment, but when 50 mg of micromotors were employed, the removal efficiency increased to 64% after 1 h.

The efficacy of the CoffeeBots in eliminating MP contaminants was examined to determine their potential for reuse. In all experiments, 50 mg of CoffeeBots were introduced in seawater and mixed with 10 mg of PS beads. Upon completion of the experiment, microrobots were using magnetically retrieved and regenerated by ethanol wash. The methods used for regeneration of CoffeeBots after MP absorption have been detailed in the ESI.† To determine the reusability of CoffeeBots for MP removal, a series of experiments was conducted wherein the microrobots were suspended into MP-polluted seawater for each subsequent repetition. The results of the study show that the microrobots maintained a removal efficiency of over ~55% after five cycles of operation (Fig. 9H). The results demonstrate the potential of microrobots for cleaning plastic contaminated seawater. The research findings further indicate that microrobots possess the ability to maintain significant efficiency even after repeated usage.

Conclusions

Herein, we report an environmentally friendly and low-cost strategy for fabricating magnetic CoffeeBots from spent coffee grounds (SCGs). These particles can effectively remove various water contaminants from seawater. We fabricated these active remediation agents for seawater detoxification from inexpensive SCGs obtained from home brewing. The commercial iron oxide nanoparticles (IONPs) were deposited non-uniformly on the hydrophobic SCG matrix to fabricate CoffeeBots. A FT-IR analysis indicates that the oxygen (O) constituents inherent in IONPs have a propensity to form enduring intermolecular hydrogen bonds with the hydroxyl functional groups present on the SCGs. The IONPs enable its remote actuation and guidance (in any desired direction) of the CoffeeBots under an external magnetic field, allowing precise control and manipulation of CoffeeBots in aqueous environ-

ments. The speed of a microrobot increases proportionately with the strength of the applied magnetic field. The external magnetic force provides a precise means for controlling the motion of either a lone CoffeeBot or a collective swarm of CoffeeBots during navigation.

Microrobots functionalized with ascorbic acid (AA) served as potent microcleaners for reducing methylene blue (MB) dye pollutants in simulated wastewater. Magnetic propulsion of CoffeeBots accelerates dye reduction in dye-contaminated seawater by enhancing fluid mixing and AA release. Furthermore, the microrobots were effective in removing oil spills and polystyrene (PS) microbeads due to their intrinsic hydrophobic nature. Using CoffeeBots to capture, transport, and retrieve hydrophobic pollutants, such as oil slicks and microplastics, makes the process more efficient. The CoffeeBots can be easily retrieved and reused after the water treatment process by using a bar magnet. In addition, the CoffeeBots are biodegradable and do not consume any toxic chemical fuels, which provides an eco-friendly strategy for the rapid elimination of water pollutants. Compared with previously reported stationary magnetic SCGs, the multifunctional motile CoffeeBots exhibit potential as a viable approach to motion-driven water treatment strategy (Table S2, refer to ESI†).

The versatility and adaptability of CoffeeBots make them well-suited for different water remediation scenarios. CoffeeBots are anticipated to serve as a customizable technology for addressing various water pollutants. One potential application is in waste stabilization ponds, which are commonly utilized in warmer climates, particularly in developing countries where coffee production is prevalent. To combat oil spills, microplastic contamination, and dye pollution in oceans, rivers, waste stabilization ponds or lakes, the CoffeeBots would be deployed from a small boat and controlled using a magnet located on board the vessel. One possible configuration (though not the only one) would be to have the magnet suspended, for example, mounted on the side of the boat and hover close to the water surface. Another possible configuration would employ CoffeeBots in a confined space by incorporating a specialized treatment tank containing a magnet on board a ship or on land (Fig. S10, refer to ESI†).[13] This water remediation system would feature a tank with an inlet pipe for contaminated water and an outlet pipe for clean water.

By combining a low-cost base material (coffee waste) that is readily abundant around the world with a straightforward synthesis process with readily-available materials, we anticipate that CoffeeBots can create novel opportunities within the realm of water purification to help resolve this urgent global need.

Experimental section

Synthesis of CoffeeBots

SCGs were Café Bustelo brand coffee grounds purchased at a local supermarket and brewed using a Bialetti Express Moka 6-Cup. After brewing, the SCGs were heated for 48 h in an oven at 105 °C, then they were ground in a mortar and pestle to obtain finer particles. To remove the remaining moisture, SCGs were further dried at 140 °C for 24 h. After this, 200 mg of dried SCGs were transferred to a 20 mL beaker. 80 mg IONPs were suspended in 6 mL of ethanol and the solution was vortexed for 30 s. The IONP solution was poured immediately into the 20 mL beaker containing SCGs and mixed with a spatula. The beaker was left undisturbed for 2 h. The solution was passed through a 100 μm strainer to obtain CoffeeBots, followed by ethanol wash to remove the unbound IONPs. The filtrate was discarded, and the residue was scooped out of the strainer, and resuspended in 10 mL beaker for final ethanol wash. The samples were magnetically retrieved from ethanol suspension and transferred to a watch glass. The watch glass was placed inside an oven at 65 °C for 24 h to evaporate the remaining ethanol and obtain dried CoffeeBots. Magnetically-responsive CoffeeBots were stored at room temperature for further use.

Synthesis of AA@CoffeeBots

200 mg of AA was dissolved in 5 mL of DI water and then 5 mL of ethanol was added to make a 10 mL of 20 mg mL^{-1} AA solution. 60 mg of CoffeeBots were placed on a watch glass and the particles were immersed in 400 μL of AA solution. Following this, the watch glass was placed in an oven at 65 °C overnight to evaporate the solvent and obtain dried sample. The AA@CoffeeBots were freshly prepared before the start of each experiment.

Magnetic control and motion characterization

Microrobots were magnetically guided in predefined trajectories using a magnet placed below the set-up, while they were suspended in a Petri dish (35 mm diameter) containing seawater. The magnet was manually moved to control microrobot motion. As a single microrobot or in swarms, CoffeeBots move along the direction of the external magnetic field. The motion was observed at room temperature under an optical microscope equipped with a CCD or smartphone camera. To evaluate the speed of the CoffeeBots, we measured their displacement from the initial point to the final position per unit of time. Microrobots were suspended in a Petri dish filled with seawater to measure velocity under magnetic influence. We performed discrete experiments with CoffeeBots of identical size to determine the mean value of speed and error bars. The speed and trajectory of the microrobots were determined from the recorded videos.

Oil remediation

Oil red O dye (0.5 mg mL^{-1}) was added to oil for better visibility of oil droplets. The oil separation efficiency (OSE) by an assembly of CoffeeBots was investigated at room temperature. To test the maximum oil absorption by CoffeeBots, a droplet of oil (25 μL) was drop-casted on a glass slide and weighed using a precise analytical balance. A definite amount of CoffeeBots (in mg) were added to 25 mg (μL) of oil, followed by a stay for 3 min. After this, the exhausted CoffeeBots were magnetically retrieved from the oil and the remnant oil slick on the glass was weighed and recorded. The OSE was determined

by the percentage of weight loss of the oil droplet from the glass slide after absorption by CoffeeBots to the initial weight of the oil. The OSE calculations and experimental procedures for microrobots regeneration reported in the ESI.†

Capture of plastic microbeads

10 mg of spherical PS microbeads (20–140 μm) were uniformly dispersed in 8 mL of seawater sample by ultrasonication. A definite mass of CoffeeBots were added to the contaminated seawater, followed by 1 h standby period. Following the treatment process, microrobots were magnetically retrieved from the solution. The treated solution was filtered using a Whatman filter paper. The filter paper was dried overnight at 80 °C to remove the water content from the remnant microbeads. To calculate the weight difference after treatment, the beads were collected and weighed using a precise analytical scale. The efficiency of removal was derived by calculating the percentage of weight loss of PS beads after treatment relative to their initial mass. The removal efficiency calculations and steps for microrobots regeneration reported in the ESI.†

Organic dye removal

Firstly, dye solution of varying concentrations ranging from 0 to 12 mg L^{-1} was prepared by dissolving the MB dye powder in seawater. The standard curve of MB dye was obtained using a microplate reader at 665 nm.

For dye removal experiments, 50 mg of AA@CoffeeBots was added to 8 mL of an MB dye solution (10 mg L^{-1} dye in seawater) in a 10 mL beaker. For each independent set of experiments, the AA@CoffeeBots were magnetically actuated inside the reaction vessel for various time intervals. After a specific time period, the magnet was placed near the beaker to trap the microrobots at one side, and 350 μL of aliquot was retrieved. The aliquot was transferred to a 1.5 mL of centrifuge tube, followed by centrifugation at 14 000 rpm for 2 min to remove suspended particles, if any. After centrifugation, 300 μL of MB solution was transferred into a 96-well microplate for absorbance analysis. The MB dye concentration was monitored by recording the absorption peak intensity at 665 nm using a microplate reader. Similarly, the additional experiments were performed for motile AA@CoffeeBots of varying amounts (10–50 mg), uncoated SCGs, CoffeeBots, stationary AA@CoffeeBots, and in absence of any particles (No SCGs). Furthermore, A description of the procedures used to regenerate microrobots can be found in the ESI.†

To observe the impact of free AA molecules, a control experiment was conducted involving the addition of 50 mg of AA@CoffeeBots to 8 mL of seawater. The mixture was allowed to settle for 1 h before retrieving the microrobots using a magnet. This process resulted in a solution containing only released AA molecules in seawater. A specific volume from a MB dye stock solution was added in the seawater to obtain a concentration of 10 mg L^{-1} dye solution. Over time, 350 μL aliquots were collected and analysed using a microplate reader to monitor the MB dye concentration at 665 nm.

Statistical analysis

The experiments were carried out in triplicate and the findings were presented as mean values with corresponding standard deviations. Graphs were generated through Origin software, while Biorender and ClipartMax was used for illustrations.

Author contributions

A. K. S. and T. B. contributed equally to the manuscript. A. K. S. and T. B. performed all the experimental investigations, analysed data, and interpreted results. J. L. M. was involved in conceptualization, supervised the research work, and assisted with data analysis. A. K. S. generated figures, edited videos, and drafted the initial version of the manuscript. The manuscript was compiled and revised through the contributions of all authors. All authors have approved the final version of the manuscript.

Conflicts of interest

All the authors are co-inventors on a provisional patent application number-63/512744 on this work.

Acknowledgements

We thank Prof. Rémi Veneziano and Prof. Lee Solomon at George Mason University (GMU) for the use of instruments in their laboratories. We acknowledge Thomas Jefferson High School for Science and Technology (TJHSST) and GMU for characterization facilities. We also extend our gratitude to Dr Brian Kennedy and Dr Dan Parilla at TJHSST for providing valuable assistance in performing FTIR operation. Contributions from Dr Chiranjit Dutta, Postdoctoral Research Fellow, GMU, are also gratefully acknowledged.

References

1 R. Kumar, M. Qureshi, D. K. Vishwakarma, N. Al-Ansari, A. Kuriqi, A. Elbeltagi and A. Saraswat, *Case Stud. Chem. Environ. Eng.*, 2022, **6**, 100219.
2 B. Petrie, R. Barden and B. Kasprzyk-Hordern, *Water Res.*, 2015, **72**, 3–27.
3 R. Al-Tohamy, S. S. Ali, F. Li, K. M. Okasha, Y. A. G. Mahmoud, T. Elsamahy, H. Jiao, Y. Fu and J. Sun, *Ecotoxicol. Environ. Saf.*, 2022, **231**, 113160.
4 P. O. Oladoye, T. O. Ajiboye, E. O. Omotola and O. J. Oyewola, *Results Eng.*, 2022, **16**, 100678.
5 S. Sangkham, O. Faikhaw, N. Munkong, P. Sakunkoo, C. Arunlertaree, M. Chavali, M. Mousazadeh and A. Tiwari, *Mar. Pollut. Bull.*, 2022, **181**, 113832.
6 T. S. M. Amelia, W. M. A. W. M. Khalik, M. C. Ong, Y. T. Shao, H. J. Pan and K. Bhubalan, *Prog. Earth Planet. Sci.*, 2021, **8**, 12.

7 T. Atugoda, M. Vithanage, H. Wijesekara, N. Bolan, A. K. Sarmah, M. S. Bank, S. You and Y. S. Ok, *Environ. Int.*, 2021, **149**, 106367.
8 Z. Asif, Z. Chen, C. An and J. Dong, *J. Mar. Sci. Eng.*, 2022, **10**, 762.
9 L. Yu, M. Han and F. He, *Arabian J. Chem.*, 2017, **10**, S1913–S1922.
10 P. Rajasulochana and V. Preethy, *Resour.-Effic. Technol.*, 2016, **2**, 175–184.
11 M. Varsha, P. Senthil Kumar and B. Senthil Rathi, *Chemosphere*, 2022, **287**, 132270.
12 S. K. Panda, N. A. Kherani, S. Debata and D. P. Singh, *Mater. Adv.*, 2023, **4**, 1460–1480.
13 M. Urso, M. Ussia and M. Pumera, *Nat. Rev. Bioeng.*, 2023, **1**, 236–251.
14 S. Hermanová and M. Pumera, *ACS Nanosci. Au*, 2022, **2**, 225–232.
15 M. Urso and M. Pumera, *Adv. Funct. Mater.*, 2022, **32**, 1–12.
16 W. Gao and J. Wang, *ACS Nano*, 2014, **8**, 3170–3180.
17 J. L. Moran and J. D. Posner, *Annu. Rev. Fluid Mech.*, 2017, **49**, 511–540.
18 R. F. Ismagilov, A. Schwartz, N. Bowden and G. M. Whitesides, *Angew. Chem., Int. Ed.*, 2002, **41**, 652–654.
19 W. F. Paxton, K. C. Kistler, C. C. Olmeda, A. Sen, S. K. St Angelo, Y. Cao, T. E. Mallouk, P. E. Lammert and V. H. Crespi, *J. Am. Chem. Soc.*, 2004, **126**, 13424–13431.
20 K. Villa and M. Pumera, *Chem. Soc. Rev.*, 2019, **48**, 4966–4978.
21 S. Palagi, D. P. Singh and P. Fischer, *Adv. Opt. Mater.*, 2019, **7**, 1–18.
22 J. Li, C. C. Mayorga-Martinez, C. D. Ohl and M. Pumera, *Adv. Funct. Mater.*, 2022, **32**, 1–27.
23 T. Bhuyan, D. Dutta, M. Bhattacharjee, A. K. Singh, S. S. Ghosh and D. Bandyopadhyay, *ACS Appl. Bio Mater.*, 2019, **2**, 4571–4582.
24 A. K. Singh, S. Rarotra, V. Pasumarthi, T. K. Mandal and D. Bandyopadhyay, *J. Mater. Chem. A*, 2018, **6**, 9209–9219.
25 X. Z. Chen, M. Hoop, F. Mushtaq, E. Siringil, C. Hu, B. J. Nelson and S. Pané, *Appl. Mater. Today*, 2017, **9**, 37–48.
26 L. Bouffier, V. Ravaine, N. Sojic and A. Kuhn, *Curr. Opin. Colloid Interface Sci.*, 2016, **21**, 57–64.
27 X. Lin, T. Si, Z. Wu and Q. He, *Phys. Chem. Chem. Phys.*, 2017, **19**, 23606–23613.
28 S. K. Srivastava, M. Guix and O. G. Schmidt, *Nano Lett.*, 2016, **16**, 817–821.
29 L. Wang, A. Kaeppler, D. Fischer and J. Simmchen, *ACS Appl. Mater. Interfaces*, 2019, **11**, 32937–32944.
30 W. Li, C. Wu, Z. Xiong, C. Liang, Z. Li, B. Liu, Q. Cao, J. Wang, J. Tang and D. Li, *Sci. Adv.*, 2022, **8**, 1–12.
31 M. Sun, W. Chen, X. Fan, C. Tian, L. Sun and H. Xie, *Appl. Mater. Today*, 2020, **20**, 100682.
32 S. G. Ullattil and M. Pumera, *Small*, 2023, **2301467**, 1–9.
33 H. Ye, Y. Wang, X. Liu, D. Xu, H. Yuan, H. Sun, S. Wang and X. Ma, *J. Colloid Interface Sci.*, 2021, **588**, 510–521.
34 A. K. Singh, T. Bhuyan, S. Maity, T. K. Mandal and D. Bandyopadhyay, *ACS Appl. Nano Mater.*, 2020, **3**, 3459–3470.
35 T. D. Minh, M. C. Ncibi, V. Srivastava, B. Doshi and M. Sillanpää, *Chemosphere*, 2021, **271**, 129516.
36 X. Li, Y. Zhao, D. Wang and X. Du, *Colloids Surf., A*, 2023, **658**, 130712.
37 S. H. Chang, *Mater. Today Sustain.*, 2022, **19**, 100196.
38 K. Wang, E. Ma and H. Wang, *Adv. Mater. Interfaces*, 2022, 2200271.
39 E. Ma, K. Wang, Z. Hu and H. Wang, *J. Colloid Interface Sci.*, 2021, **603**, 685–694.
40 L. Dekanovsky, H. Huang, S. Akir, Y. Ying, Z. Sofer and B. Khezri, *Small Methods*, 2023, 2201547.
41 J. Tesař, M. Ussia, O. Alduhaish and M. Pumera, *Appl. Mater. Today*, 2022, **26**, 101312.
42 L. Dekanovsky, B. Khezri, Z. Rottnerova, F. Novotny, J. Plutnar and M. Pumera, *Nat. Mach. Intell.*, 2020, **2**, 711–718.
43 V. V. Singh, K. Kaufmann, B. E.-F. de Ávila, M. Uygun and J. Wang, *Chem. Commun.*, 2016, **52**, 3360–3363.
44 D. Vilela, M. M. Stanton, J. Parmar and S. Sánchez, *ACS Appl. Mater. Interfaces*, 2017, **9**, 22093–22100.
45 K. Johnson, Y. Liu and M. Lu, *Front. Chem. Eng.*, 2022, **4**, 838605.
46 L. F. Ballesteros, J. A. Teixeira and S. I. Mussatto, *Food Bioprocess Technol.*, 2014, **7**, 3493–3503.
47 D. Pujol, C. Liu, J. Gominho, M. À. Olivella, N. Fiol, I. Villaescusa and H. Pereira, *Ind. Crops Prod.*, 2013, **50**, 423–429.
48 K. T. Lee, C. L. Cheng, D. S. Lee, W. H. Chen, D. V. N. Vo, L. Ding and S. S. Lam, *Energy*, 2022, **239**, 122467.
49 L. Acosta, D. Galeano-Caro, O. E. Medina, F. B. Cortés and C. A. Franco, *Processes*, 2021, **9**, 63.
50 M. F. Rizkiana, Hidayatullah, A. Rosalina, B. A. Fachri and H. Harada, *IOP Conf. Ser.: Mater. Sci. Eng.*, 2021, **1053**, 012007.
51 N. Hussain, S. Chantrapromma, T. Suwunwong and K. Phoungthong, *Mater. Res. Express*, 2020, **7**, 085503.
52 M. S. Akindolie and H. J. Choi, *Water Sci. Technol.*, 2022, **85**, 1218–1234.
53 F. J. Cerino-Córdova, P. E. Díaz-Flores, R. B. García-Reyes, E. Soto-Regalado, R. Gómez-González, M. T. Garza-González and E. Bustamante-Alcántara, *Int. J. Environ. Sci. Technol.*, 2013, **10**, 611–622.
54 J. C. Silva, G. E. Oliveira, R. D. Toledo Filho and F. G. Souza, *Macromol. Symp.*, 2018, **380**, 1–6.
55 F. Taleb, M. Ammar, M. ben Mosbah, R. ben Salem and Y. Moussaoui, *Sci. Rep.*, 2020, **10**, 1–13.
56 L. Hao, P. Wang and S. Valiyaveettil, *Sci. Rep.*, 2017, **7**, 42881.
57 M. A. Ahsan, M. T. Islam, M. A. Imam, A. H. M. G. Hyder, V. Jabbari, N. Dominguez and J. C. Noveron, *J. Environ. Chem. Eng.*, 2018, **6**, 6602–6611.
58 Y. Dai, K. Zhang, X. Meng, J. Li, X. Guan, Q. Sun, Y. Sun, W. Wang, M. Lin, M. Liu, S. Yang, Y. Chen, F. Gao, X. Zhang and Z. Liu, *Chemosphere*, 2019, **215**, 163–172.

59 P. L. Yen, C. H. Hsu, M. L. Huang and V. H. C. Liao, *Chemosphere*, 2022, **286**, 131863.
60 H. Firomesa, M. Amde, D. Bekana and A. Temesgen, *Chem. Pap.*, 2022, **76**, 2267–2277.
61 H. Farhid and A. Shaabani, *J. Iran. Chem. Soc.*, 2021, **18**, 1199–1209.
62 A. A. Edathil, I. Shittu, J. Hisham Zain, F. Banat and M. A. Haija, *J. Environ. Chem. Eng.*, 2018, **6**, 2390–2400.
63 S. Asliyüce Çoban, I. Safarik and A. Denizli, *Turk. J. Chem.*, 2021, **45**, 157–166.
64 N. Besharati, N. Alizadeh and S. Shariati, *J. Mex. Chem. Soc.*, 2018, **62**, 110–124.
65 A. Zuorro and R. Lavecchia, *Appl. Mech. Mater.*, 2013, **394**, 3–7.
66 M. Rahmayanti, S. J. Santosa and S. Sutarno, *J. Bahan Alam Terbarukan*, 2020, **9**, 81–87.
67 M. Takasuka, M. Kishi and M. Yamakawa, *J. Med. Chem.*, 1994, **37**, 47–56.
68 A. Sanchis, G. Prolongo and G. Rubio, *Polym. J.*, 1995, **27**, 10–20.
69 S. Ebbens, D. A. Gregory, G. Dunderdale, J. R. Howse, Y. Ibrahim, T. B. Liverpool and R. Golestanian, *EPL*, 2014, **106**, 58003.
70 W. Gao, A. Pei and J. Wang, *ACS Nano*, 2012, **6**, 8432–8438.
71 A. Brown and W. Poon, *Soft Matter*, 2014, **10**, 4016–4027.
72 W. F. Paxton, P. T. Baker, T. R. Kline, Y. Wang, T. E. Mallouk and A. Sen, *J. Am. Chem. Soc.*, 2006, **128**, 14881–14888.
73 Z. Benmaamar, H. Boutoumi, H. Hamitouche, H. Benmaamar, S. Mazari, A. Benmaamar, A. Benmaamar, S. Semsari and A. Aggoun, *International Journal of Multidisciplinary Sciences*, 2016, **1**, 10–29.
74 A. A. Ayalew and T. A. Aragaw, *Adsorpt. Sci. Technol.*, 2020, **38**, 205–222.
75 Q. A. Trieu, H. D. Nguyen and T. H. Bui, *AIP Conf. Proc.*, 2022, **2610**, 040013.
76 H. J. El-Aila, *Tenside, Surfactants, Deterg.*, 2012, **49**, 26–31.
77 S. Mowry and P. J. Ogren, *J. Chem. Educ.*, 1999, **76**, 970–974.
78 P. E. Strizhak, *Theor. Exp. Chem.*, 1994, **29**, 283–284.
79 H. Lund and H. Lieck, *Skand. Arch. Physiol.*, 1936, **74**, 269–271.
80 A. M. Butler, M. Cushman and E. A. MacLachlan, *J. Biol. Chem.*, 1943, **150**, 453–461.
81 A. Jancik-Prochazkova, C. C. Mayorga-Martinez, J. Vyskočil and M. Pumera, *ACS Appl. Mater. Interfaces*, 2022, **14**, 45545–45552.
82 W. Gao, X. Feng, A. Pei, Y. Gu, J. Li and J. Wang, *Nanoscale*, 2013, **5**, 4696–4700.
83 G. Shi, M. Wu, Q. Zhong, P. Mu and J. Li, *Langmuir*, 2021, **37**, 7843–7850.
84 H. Li, Q. Zhong, Q. Sun, B. Xiang and J. Li, *Langmuir*, 2022, **38**, 3493–3500.
85 Q. Zhong, Q. Sun, B. Xiang, P. Mu, W. Guo and J. Li, *Colloids Surf., A*, 2023, **674**, 131868.
86 L. Wang and K. Villa, *Environ. Sci. Nano*, 2021, **8**, 3440–3451.